Laser Action in the Stellar Atmospheres of Wolf-Rayet Stars and Quasi-Stellar Objects (QSOs)

Pierre A. Millette
E-mail: pierre.millette@uottawa.ca, Ottawa, Canada

In this paper, we reconsider the little-known but critically important physical process of laser action occurring in the stellar atmospheres of Wolf-Rayet stars and, by extension, of QSOs, also known as quasars in the cosmological context. We review the use of the Collisional-Radiative (non-LTE) model for hydrogenic and lithium-like ions to calculate the energy level populations and the existing results for He I, He II, C III and C IV, and for N V and O VI. We review the details of laser action in Wolf-Rayet stars, as well as in QSOs. We note that taking QSOs to be local stellar objects eliminates the problems associated with their cosmological interpretation. We propose that the terminology *quasar* be used to refer to the cosmological interpretation and *QSO* to refer to the stellar interpretation of Quasi-Stellar Objects. We introduce a new star type Q for QSOs, similar to the star type W for Wolf-Rayet stars. We expand the Hertzsprung-Russell diagram to include more massive and hotter stars of type Q and W beyond the stars of type O B. The main sequence thus starts with stars of type Q W O B, followed by the rest of the main sequence. Finally, we note the effort that will be required to understand the classification and evolution of stars of type Q, as has been achieved for Wolf-Rayet stars.

1 Introduction

In this paper, we reconsider a little-known but critically important physical process occurring in the stellar atmospheres of Wolf-Rayet stars and, by extension, of Quasi-Stellar Objects (QSOs), also known as quasars in the cosmological context. Wolf-Rayet stars are known to have an expanding envelope of hot ionized gases, as the stellar atmosphere of the star expands, resulting in mass loss.

If the speed of expansion is low, the expansion will be closer to being isothermal, but as the speed of expansion increases, the expansion will become adiabatic. Under those conditions, as the plasma cools, population inversions will occur in the ionic energy levels due to free electron-ion recombination in higher ionic excited states. Some ionic energy level transitions will undergo laser action [1] resulting in spectra dominated by a small number of strong broad emission lines, which becomes even more evident in QSOs.

2 Wolf-Rayet stars

Wolf-Rayet stars [2] are a type of stars that, like the supergiants, have extended atmospheres whose thickness is an appreciable fraction of their stellar radius [3, p. 243]. Characteristic features in the visible spectra of many O and early B stars, particularly supergiants, and WR stars provide evidence that these objects have extensive envelopes, and that the material generating the lines is flowing outward from the stellar photosphere.

The number of WR stars in our galaxy is small: the 2001 VIIth catalog of galactic WR stars gave the number at 227 stars, comprised of 127 WN stars, 87 WC stars, 10 WN/WC stars and 3 WO stars [4]. The subtypes are covered in the spectra discussion later in this section. A 2006 update added another 72 WR stars, including 45 WN stars, 26 WC stars and one WO star [5]. The latest number from the August 2020 Galactic Wolf Rayet Catalogue v1.25 is 667 WR stars [6].

The existence of large-scale, rapid, and sometimes violent expansions of stellar atmospheres is well-established observationally [3, p. 471]. Beals [7, 8] first recognized that the great breadths of lines in WR spectra, indicating velocities of the order of 3 000 km/s, could be interpreted in terms of rapid outflow of material. His suggestion that the flow was driven by radiation pressure is supported by current dynamical models. Further evidence for mass loss is provided by infrared and radio continuum observations of several OB and WR stars, which are most readily interpreted in terms of free-free emission from an extended, optically-thick envelope having a density profile consistent with steady outflow of the stellar atmosphere [3, p. 550–551].

We know today, from a variety of observational evidence from spacecraft and ground-based observatories, that in the WR and Of stars and in many early-type supergiants, there are massive trans-sonic stellar winds, that have very small outward velocities in the deeper layers of the stars, but a large outward acceleration producing very large velocities ($v/c \approx 0.01$) at great distances from the stars [3, pp. 471–472,550]. These flows are driven by radiation pressure acting on the stellar atmosphere [3, p. 523].

Mass loss in stellar winds, particularly in the early-type OB supergiants and WR stars, is well established [3, pp. 266, 523]. The analysis of line profiles and infrared emissions imply estimated mass loss rates $\mathcal{M}$ of order 10^{-6} to 10^{-5} $\mathcal{M}_\odot$/year for O stars and perhaps up to 10^{-4} $\mathcal{M}_\odot$/year for

WR stars [9, p. 628]. For comparison, mass loss rates for the solar wind is about 10^{-14} $\mathcal{M}_\odot$/year. The flow velocities rise from close to zero in the stellar photosphere to highly supersonic values within one stellar radius from the surface. The 3 000 km/s flow is thought to be driven by momentum input to the ionized gas from the intense radiation force exerted by the strong spectrum lines of these extremely luminous stars.

Series of extremely strong emission lines can be observed in the spectra of WR stars. The spectra fall into two broad classes: WN, which have prominent lines of nitrogen N and helium He ions, with a very strong He II Pickering series ($n = 4 \rightarrow n'$), and essentially no lines of carbon C; and WC, where the lines of carbon C and oxygen O are prominent along with the helium He ions, while those of nitrogen N seem to be practically absent [3, p. 485]. An additional subtype WO with strong O VI lines has also recently been added as a separate subtype. The spectra are characterized by the dominance of emission lines, notable for the almost total absence of hydrogen H lines [10].

3 Laser action in stellar atmospheres

In initial modelling calculations, Castor [11] used the escape probability method of basic Sobolev theory to treat the transfer of line radiation in a stellar envelope to provide a coarse analysis of the spectral line formation in Wolf-Rayet stars for a line formed in a two-level atom [3, p. 471–472]. He then used this analysis to calculate the populations of the first thirty levels of hydrogen-like He II ions under statistical equilibrium with all radiative and collisional transitions included [12]. He also applied this analysis to 14 terms and all allowed transitions of helium-like C III ions; no case of laser action was found in the calculations as the existing atomic processes used did not provide sufficient pumping of the excited levels to maintain population inversion [13].

Mihalas [3, p. 485–490] carries out a complete multilevel analysis of the spectrum of an ion using statistical equilibrium equations that consider the radiative and collisional processes contributing to the population of each ionic level under consideration. Typically, the only free parameters in this analysis are T_e, the temperature of the free electrons corresponding to the envelope temperature, n_e, the free electron number density and n_{atom}, the total number density of the species (element) under consideration. The analysis is done under Local Thermodynamic Equilibrium (LTE) conditions, that is under conditions in which each volume element of the plasma fulfills all thermodynamic equilibrium laws derived for plasmas in complete thermodynamic equilibrium (CTE) except for Planck's radiation law [40, p. 12–13].

3.1 Plasma lasers

The possibility of using a recombining plasma as an amplifying medium of electromagnetic radiation was first suggested by Gudzenko and Shelepin [14]. Calculations performed on a hydrogen plasma [15, 17] subsequently confirmed this suggestion. Such plasmas are called plasma lasers [18].

We consider the basic principles of operation of a plasma laser. The mean time between electron collisions determines the rate of establishment of the electron temperature within a plasma. The smallness of the time between elastic collisions in a dense plasma thus makes it possible, in principle, to rapidly reduce the electron temperature of such a plasma. For example, in plasma densities of order $n_i \sim n_e \sim 10^{15} - 10^{16}\,\mathrm{cm}^{-3}$, a single distribution of the electrons is established in a time of order $\tau \sim 10^{-11} - 10^{-10}$ s [14], where n_i is the ion number density.

Rapid cooling of a strongly ionized plasma results in rapid recombination of the electrons and the ions into highly excited ionic states. The subsequent relaxation of the electrons to the ground state by spontaneous and non-radiative transitions occurs in a time which, for the estimated values of the plasma parameters used in this work, is larger than 10^{-7} s. At those densities, electron-ion recombination occurs by three-body recombination in a time shorter than 10^{-7} s such that a rapid filling-up of the upper excited levels of the ions occurs. Furthermore, since recombination into highly excited states occurs much more rapidly than into lower states, the establishment of large population inversions is favored.

When large population inversions have been established in the excited levels, the plasma is said to be in a stationary drainage state. It is still substantially ionized. As an example of the time involved, Gudzenko et al. [15] find that for a dense low temperature plasma ($T_e \sim 1000 - 6000$ K and n_e-bound and free states $\sim 10^{13} - 10^{16}\,\mathrm{cm}^{-3}$), cooled by a factor of twenty, stationary drainage of the excited discrete levels is established in a time $\sim 10^{-8} - 10^{-7}$ s. Stationary drainage is maintained for a time $\sim 10^{-5}$ s, and is followed by a stage in which the plasma is weakly ionized and the population densities of its levels return to normal. Gudzenko et al. [17] find that the above conditions can be significantly relaxed; for example, the cooling can be done more slowly or by stages [40, p. 42–43].

3.2 Adiabatic cooling of a plasma

Various mechanisms of free electron cooling can be used. The method of interest to us, rapid cooling of a plasma by adiabatic expansion, was first investigated by Gudzenko et al. [16] both for magnetized and unmagnetized plasmas.

An example of this cooling mechanism is the adiabatic expansion of a plasma jet in a vacuum. The advantage of this method is that continuous amplification, and thus continuous operation of a laser is possible due to the fact that the different stages of the recombining plasma decay at different times. Thus, as the plasma expands, the stages of the recombination process outlined in the previous Section §3.1 are spread over space and the de-excited medium is thus removed from the active lasing zone. Experimental evidence

of laser action due to the adiabatic expansion of highly ionized hydrogen or hydrogenic plasmas has been given by, for example, [19] and [20].

Under adiabatic expansion conditions, the density n and the temperature T of a gas are related by [17]

$$T\, n^{1-\gamma} = \text{constant} \tag{1}$$

where

$$\gamma = c_P/c_V \tag{2}$$

is the ratio of the specific heat at constant pressure c_P and the specific heat at constant volume c_V. For a monatomic gas and for a fully ionized plasma of hydrogen, we use [17]

$$\gamma = 5/3\,. \tag{3}$$

However, it should be noted that the actual value of γ for a plasma is slightly smaller than 5/3. Denoting the initial density and temperature of the plasma by n_0 and T_0 respectively, and the final density and temperature by n and T respectively, we characterize the expansion by the factor

$$f_E = \frac{n_0}{n} > 1 \tag{4}$$

and the ensuing cooling of the plasma by the factor

$$f_C = \frac{T_0}{T} > 1\,. \tag{5}$$

Then from (1), we have the relation

$$f_C = f_E^{\gamma-1} \tag{6}$$

under adiabatic expansion conditions. In this work, we use $f_c = 5$; then from (6) and (3), $f_E = 11.2$ [40, p. 43–44].

4 The Collisional-Radiative (non-LTE) model

To calculate the non-equilibrium population of the ionic energy levels, we need to use a model that applies to non-LTE plasmas. The Collisional-Radiative (CR) non-LTE model was first proposed and applied to hydrogenic ions by Bates et al. [21,22] and subsequently used by Bates and Kingston [23] and McWhirter and Hearn [24]. It was first applied to helium by Drawin and Emard [25], to lithium by Gordiets et al. [26], and to cesium by Norcross and Stone [27].

The population densities of the energy levels of ions in non-LTE plasmas must be obtained from the rate coefficients of the individual collisional and radiative processes occurring within the plasma, as summarized in Fig. 1. The physical processes included in the CR model include:

- Collisional ionization by electron impact
  Rate coefficient: $S_p(T)\,\mathrm{cm^3 s^{-1}}$
  Number of processes: $n_p\, n_e\, S_p(T)\,\mathrm{cm^{-3} s^{-1}}$
- Three-body recombination
  Rate coefficient: $\alpha_p(T)\,\mathrm{cm^6 s^{-1}}$
  Number of processes: $n_e^2\, n_i\, \alpha_p(T)\,\mathrm{cm^{-3} s^{-1}}$

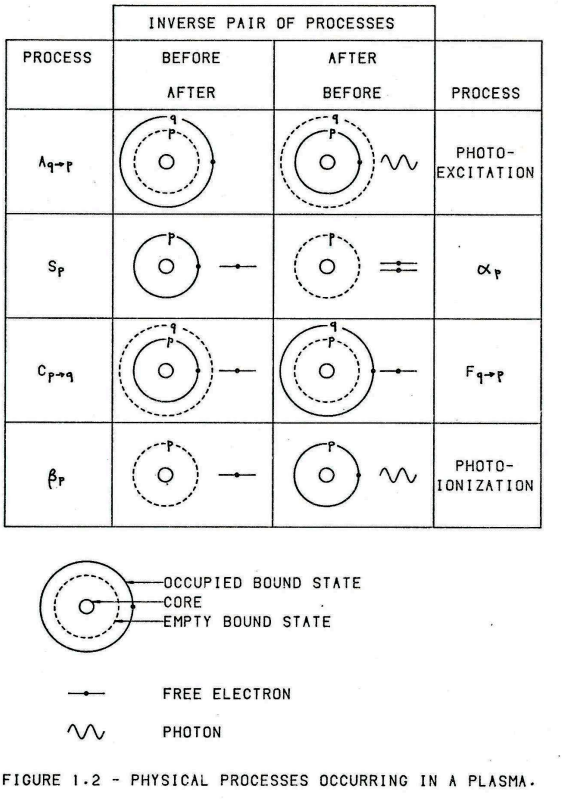

Fig. 1: This figure provides a summary of the collisional and radiative processes occurring within the plasma, where p and q are ionic energy state labels; $p \gtrless q$ [40, p. 21].

- Radiative recombination
  Rate coefficient: $\beta_p(T)\,\mathrm{cm^3 s^{-1}}$
  Number of processes: $n_e\, n_i \beta_p(T)\,\mathrm{cm^{-3} s^{-1}}$
- Collisional excitation by electron impact ($p < q$)
  Rate coefficient: $C_{p\to q}(T)\,\mathrm{cm^3 s^{-1}}$
  Number of processes: $n_p\, n_e\, C_{p\to q}(T)\,\mathrm{cm^{-3} s^{-1}}$
- Collisional de-excitation by electron impact ($p < q$)
  Rate coefficient: $F_{q\to p}(T)\,\mathrm{cm^3 s^{-1}}$
  Number of processes: $n_q\, n_e\, F_{q\to p}(T)\,\mathrm{cm^{-3} s^{-1}}$
- Spontaneous transition ($p < q$)
  Rate coefficient: $A_{q\to p}\,\mathrm{s^{-1}}$
  Number of processes: $n_q\, A_{q\to p}\,\mathrm{cm^{-3} s^{-1}}$

The plasma is assumed to be optically thin such that all radiation emitted within the plasma escapes without being absorbed. The following physical processes are thus neglected:

- Photoexcitation ($p < q$),
- Photoionization.

The differential equation describing the time variation of the population density of a given ionic level p is then given

by

$$\frac{dn_p}{dt} = (\text{electrons entering level } p) - \\ - (\text{electrons leaving level } p) \,. \tag{7}$$

The terms of (7) in parentheses include contributions from all levels $q < p$, $q > p$, and continuum states. Substituting for the collisional and radiative processes considered above, we obtain the differential equation

$$\begin{aligned} \dot{n}_p = & \sum_{q=1}^{p-1} C_{q\to p}\, n_e\, n_q - \\ & - \left[\left(\sum_{q=1}^{p-1} F_{p\to q} + S_p + \sum_{q=p+1}^{\infty} C_{p\to q}\right) n_e + \sum_{q=1}^{p-1} A_{p\to q}\right] n_p + \\ & + \sum_{q=p+1}^{\infty} \left(F_{q\to p}\, n_e + A_{q\to p}\right) n_q + \\ & + \left(\alpha_p\, n_e + \beta_p\right) n_e\, n_i \end{aligned} \tag{8}$$

where the dot over n_p represents differentiation with respect to time. There is such an equation for each and every level $p = 1, 2, ..., \infty$ of the ion. We thus obtain an infinite number of coupled first order differential equations in the population densities of the discrete levels of the ion.

The population density of level p, n_p, is normalized with the Saha equilibrium population density of level p, n_p^E, [28, p. 154] [29, p. 135]

$$\rho_p = \frac{n_p}{n_p^E} \,, \tag{9}$$

with n_p^E given by

$$n_p^E = Z_p(T)\, n_i\, n_e \,, \tag{10}$$

where

$$Z_p(T) = \frac{\omega_p}{u_i} \frac{h^3}{2(2\pi mkT)^{3/2}}\, e^{I_p/kT} \,, \tag{11}$$

ω_p is the statistical weight of level p, u_i is the ionic partition function, and I_p is the ionization potential of state p. For hydrogenic ions, u_i is the partition function of the bare nucleus and is given by $u_i \simeq 1$. The same holds for lithium-like ions since u_i is then the partition function of a closed shell ion.

The relative population densities of various stages of ionization n_i of a monatomic non-LTE plasma under statistical equilibrium are calculated approximately with the model of House [30]. Even though the calculations are highly simplified, the model provides a first approximation to the ionization equilibrium of monatomic plasmas of hydrogen to iron and a general method of obtaining a consistent set of relative population densities for the ionization stages of these elements.

Given that there exists a high-lying quantum state r above which the discrete levels are in LTE, the normalization (9) allows us to set the population density of these levels to be given by $\rho_{p>r} = 1$. The infinite set of equations (8) thus becomes a finite set of r coupled equations which can be solved for ρ_p, $p = 1, 2, ..., r$. The infinite sums appearing in (8) can be cut off at a sufficiently high-lying level $s > r$ above which the rate coefficients involving these states contribute little to the infinite sums of (8). For levels in LTE, detailed balancing between the collisional excitation and de-excitation processes holds and then we can use

$$n_q^E\, F_{q\to p} = n_p^E\, C_{p\to q} \,. \tag{12}$$

The set of equations (8) then becomes

$$\begin{aligned} \dot{\rho}_p = & \sum_{q=1}^{p-1} F_{p\to q}\, n_e\, \rho_q - \\ & - \left[\left(\sum_{q=1}^{p-1} F_{p\to q} + S_p + \sum_{q=p+1}^{s} C_{p\to q}\right) n_e + \sum_{q=1}^{p-1} A_{p\to q}\right] \rho_p + \\ & + \sum_{q=p+1}^{r} \left(C_{p\to q}\, n_e + \frac{Z_q}{Z_p} A_{q\to p}\right) \rho_q + \frac{1}{Z_p}\left(\alpha_p\, n_e + \beta_p\right) + \\ & + \sum_{q=r+1}^{s} \left(C_{p\to q}\, n_e + \frac{Z_q}{Z_p} A_{q\to p}\right) ; p = 1, 2, ..., r \,. \end{aligned} \tag{13}$$

4.1 Solution of the system of coupled differential equations

The exact solution of the system of couple differential equations (13) gives the time evolution of the population densities of the ionic levels $\rho_p(t)$, $p = 1, 2, ..., r$. This solution if of limited use. A simpler solution, known as the quasi-steady state (QSS) approximation, holds for a large class of plasmas and is used extensively in the literature (see [21, 22] and subsequent papers mentioned previously in §4). The steady state (SS) solution is obtained by putting

$$\dot{\rho}_p^{SS}(t) = 0 \,; p = 1, 2, ..., r \,. \tag{14}$$

This time-independent solution holds when the rate at which the electrons enter level p equals the rate at which they leave level p. Once the steady state solution is established, a perturbation of the population density of level p will be followed by a return to its steady state value in a time of order

$$\tau_p \sim \left\{\left[\sum_{q=1}^{p-1} F_{p\to q} + S_p + \sum_{q=p+1}^{s} C_{p\to q}\right] n_e + \sum_{q=1}^{p-1} A_{p\to q}\right\}^{-1} \tag{15}$$

where τ_p is the relaxation time of level p.

McWhirter and Hearn [24] have calculated τ_p for a wide range of plasma parameters. They conclude that the relaxation time of the ground state is always much greater than that of any of the excited states, even if the plasma is not

near its steady state. This is due to two main reasons: a) the electron collision rate coefficients between excited states are much greater than those involving the ground state; b) the ground state cannot decay by spontaneous radiative transition. Consequently, the population densities of the excited ionic levels come into equilibrium with particular values of the population densities of the ground state, of the free electrons, and of the ions in a time which is very short as compared to the ground state relaxation time. This is the basis of the QSS solution.

4.2 The population coefficients

We thus express the population densities of the excited states as a function of the ground state population density:

$$\rho_p = r_p^{(0)} + r_p^{(1)} \rho_1 \, ; p = 2, 3, ..., r \, . \tag{16}$$

$r_p^{(0)}$ and $r_p^{(1)}$ are called the population coefficients of level p. Furthermore, since the population densities of the excited states are in equilibrium with that of the ground state, we solve the system of coupled equations (13) by putting $\dot{\rho}_{p\geq 2} = 0$ and $\dot{\rho}_1 \neq 0$ since, in general, the ground state is not in equilibrium. In our calculations, we also assume that the free electron and ionic densities, n_e and n_i respectively, do not change substantially during the time of establishment of the QSS.

Substituting the trial solution (16) in the system of equations (13), we obtain a set of equations of the form

$$a_p + b_p \rho_1 = 0 \, ; p = 2, 3, ..., r \, . \tag{17}$$

The general solution of (17), for an arbitrary value of ρ_1, is $a_p = 0$ and $b_p = 0$. Before proceeding with the solution, certain limiting conditions must be imposed on the population coefficients $r_p^{(0)}$ and $r_p^{(1)}$ corresponding to the cases when $p = 1$ and $p > r$. Substituting $p = 1$ in (16), we obtain the condition $r_1^{(0)} = 0$ and $r_1^{(1)} = 1$. The other condition, which is obtained by putting $p > r$ in (16), has already been imposed on the set of equations, namely $r_{p>r}^{(0)} = 1$ and $r_{p>r}^{(1)} = 0$.

Using these conditions, we obtain the following two sets of $r - 1$ equations in the population coefficients $r_p^{(0)}$ and $r_p^{(1)}$ respectively:

$$\begin{aligned} &\sum_{q=2}^{p-1} F_{p\to q}\, n_e\, r_q^{(0)} - \\ &- \left[\left(\sum_{q=2}^{p-1} F_{p\to q} + S_p + \sum_{q=p+1}^{s} C_{p\to q} \right) n_e + \sum_{q=1}^{p-1} A_{p\to q} \right] r_p^{(0)} + \\ &+ \sum_{q=p+1}^{r} \left(C_{p\to q}\, n_e + \frac{Z_q}{Z_p} A_{q\to p} \right) r_q^{(0)} = -\frac{1}{Z_p} \left(\alpha_p\, n_e + \beta_p \right) - \\ &- \sum_{q=r+1}^{s} \left(C_{p\to q}\, n_e + \frac{Z_q}{Z_p} A_{q\to p} \right) ; \end{aligned} \tag{18}$$

$$\begin{aligned} &\sum_{q=2}^{p-1} F_{p\to q}\, n_e\, r_q^{(1)} - \\ &- \left[\left(\sum_{q=1}^{p-1} F_{p\to q} + S_p + \sum_{q=p+1}^{s} C_{p\to q} \right) n_e + \sum_{q=1}^{p-1} A_{p\to q} \right] r_p^{(1)} + \\ &+ \sum_{q=p+1}^{r} \left(C_{p\to q}\, n_e + \frac{Z_q}{Z_p} A_{q\to p} \right) r_q^{(1)} = \\ &= -F_{p\to 1}\, n_e \, ; p = 2, 3, ..., r \, . \end{aligned} \tag{19}$$

4.3 The population densities

Once the population coefficients $r_p^{(0)}$ and $r_p^{(1)}$ have been obtained from the sets of equations (18) and (19) respectively, they are substituted in (16). For any value of ρ_1, the population densities ρ_p can then be calculated. From (9) and (10),

$$\rho_p = \frac{n_p}{Z_p\, n_i\, n_e} \, ; \tag{20}$$

substituting (20) in (16), we obtain

$$n_p = Z_p\, n_i\, n_e\, r_p^{(0)} + \frac{Z_p}{Z_1}\, n_1\, r_p^{(1)} \, ; p = 2, 3, ..., r \, . \tag{21}$$

As required by the QSS approximation, the population density of the excited state p depends on the value of the ground state population density n_1, the free electron density n_e, and the ionic density n_i. The population density per unit statistical weight is given by $y_p = n_p/\omega_p$, where ω_p is the statistical weight of level p. The population density per unit statistical weight must be used when the population densities of different states are compared.

4.4 The collisional-radiative rate coefficients

The time evolution of the population density of the ground state can be studied with (13) when $p = 1$. Substituting for ρ_p from (16), and using the previously calculated population coefficients and (9), we obtain the differential equation

$$\dot{n}_1 = -S_{CR}\, n_e\, n_1 + \alpha_{CR}\, n_e\, n_i \, . \tag{22}$$

S_{CR} and α_{CR} are called the collisional-radiative ionization and recombination rate coefficients respectively. They are the effective ionization and recombination rate coefficients of the plasma. They are related to the individual atomic rate coefficients by the following expressions:

$$\begin{aligned} S_{CR} = S_1 + \sum_{q=2}^{s} C_{1\to q} - \\ - \frac{1}{Z_1\, n_e} \sum_{q=2}^{s} Z_q \left(F_{q\to 1}\, n_e + A_{q\to 1} \right) r_q^{(1)} \, ; \end{aligned} \tag{23}$$

$$\alpha_{CR} = \alpha_1\, n_e + \beta_1 + \sum_{q=2}^{s} Z_q \left(F_{q\to 1}\, n_e + A_{q\to 1} \right) r_q^{(0)} \, . \tag{24}$$

The solution of (22) can easily be shown to be given by

$$n_1(t) = \frac{\alpha_{CR}}{S_{CR}}\, n_i + \left(n_1(t=0) - \frac{\alpha_{CR}}{S_{CR}}\, n_i \right) e^{-S_{CR}\, n_e\, t} . \qquad (25)$$

The steady state population density of the ground state is obtained in the limit $t \to \infty$:

$$n_1^{SS} = \frac{\alpha_{CR}}{S_{CR}}\, n_i . \qquad (26)$$

4.5 Modifications for lithium-like ions

The CR model must be modified to account for the difference in structure of lithium-like and hydrogenic ions considered previously. The same system of state labelling is used: the ground state ($2s$) is labelled 1, the first excited state ($2p$) is labelled 2, the second excited state ($3s$) is labelled 3, and so on in order of increasing level energy. The derivation of the equations of the CR plasma model for lithium-like ions then parallels that given previously for hydrogenic ions.

The time evolution of the population density of level p in an optically thin plasma is given by (13) as before. The steady state (SS) solution to the set of coupled first order differential equations (13) is obtained as before from (14). However, the quasi-steady state (QSS) solution must be modified to account for the small energy separation of the ground and the first excited states as compared to that of the first and the second excited states, as this is particularly significant for ions with large values of Z such as C IV, N V, and O VI. As a result of this, the population density of the first excited state (level 2) is very much larger than that of the other excited states, and it may even be comparable to that of the ground state.

Consequently, the QSS solution is modified by using a method similar to the one developed by Bates et al. [22] to describe hydrogenic plasmas optically thick toward the lines of the Lyman series. The normalized population density of level p is expressed as a function of the ground and the first excited state population densities:

$$\rho_p = r_p^{(0)} + r_p^{(1)}\, \rho_1 + r_p^{(2)}\, \rho_2 \qquad (27)$$

where $3 \le p \le r$ and $r_p^{(0)}$, $r_p^{(1)}$ and $r_p^{(2)}$ are the population coefficients of level p. The QSS solution is obtained when the population densities of the second and higher excited states are in equilibrium with the population densities of the ground and the first excited states which, in general, are not in equilibrium. We then have $\dot{\rho}_1(t) \neq 0$, $\dot{\rho}_2(t) \neq 0$, and $\dot{\rho}_{p\ge 3}(t) = 0$.

Substituting the solution (27) in the system of equations (13), and using the last condition above, we obtain a set of equations of the form

$$a_p + b_p\, \rho_1 + c_p\, \rho_2 = 0\,;\, p = 3, 4, ..., r\,. \qquad (28)$$

For arbitrary values of ρ_1 and ρ_2, the general solution of (28) is given by $a_p = 0$, $b_p = 0$, and $c_p = 0$. We must also impose the limiting conditions corresponding to the values of $p = 1, 2$ and $p > r$ on the population coefficients $r_p^{(0)}$, $r_p^{(1)}$ and $r_p^{(2)}$: $r_1^{(0)} = 0$, $r_1^{(1)} = 1$, $r_1^{(2)} = 0$; $r_2^{(0)} = 0$, $r_2^{(1)} = 0$, $r_2^{(2)} = 1$; $r_{p>r}^{(0)} = 1$, $r_{p>r}^{(1)} = 0$, $r_{p>r}^{(2)} = 0$. This last condition has already been applied to derive the system of equations (13).

Using these conditions, we obtain three sets of $r-2$ equations which are solved for the population coefficients $r_p^{(0)}$, $r_p^{(1)}$ and $r_p^{(2)}$ respectively:

$$\sum_{q=3}^{p-1} \mathcal{A}_{pq}\, r_q^{(0)} - \mathcal{B}_p\, r_p^{(0)} + \sum_{q=p+1}^{r} C_{pq}\, r_q^{(0)} = -\frac{1}{Z_p}\left(\alpha_p\, n_e + \beta_p\right) - \sum_{q=r+1}^{s} \left(C_{p\to q}\, n_e + \frac{Z_q}{Z_p}\, A_{q\to p} \right); \qquad (29)$$

$$\sum_{q=3}^{p-1} \mathcal{A}_{pq}\, r_q^{(1)} - \mathcal{B}_p\, r_p^{(1)} + \sum_{q=p+1}^{r} C_{pq}\, r_q^{(1)} = -F_{p\to 1}\, n_e\,; \qquad (30)$$

$$\sum_{q=3}^{p-1} \mathcal{A}_{pq}\, r_q^{(2)} - \mathcal{B}_p\, r_p^{(2)} + \sum_{q=p+1}^{r} C_{pq}\, r_q^{(2)} = -F_{p\to 2}\, n_e \qquad (31)$$

where

$$\mathcal{A}_{pq} = F_{p\to q}\, n_e\,; \qquad (32)$$

$$\mathcal{B}_p = \left(\sum_{q=1}^{p-1} F_{p\to q} + S_p + \sum_{q=p+1}^{s} C_{p\to q} \right) n_e + \sum_{q=1}^{p-1} A_{p\to q}\,; \qquad (33)$$

$$C_{pq} = C_{p\to q}\, n_e + \frac{Z_q}{Z_p}\, A_{q\to p}\,;\, p = 3, 4, ..., r\,. \qquad (34)$$

From the population coefficients $r_p^{(0)}$, $r_p^{(1)}$ and $r_p^{(2)}$, the population densities n_p can be calculated for any value of n_1 and n_2 from

$$n_p = Z_p\, n_i\, n_e\, r_p^{(0)} + \frac{Z_p}{Z_1}\, n_1\, r_p^{(1)} + \frac{Z_p}{Z_2}\, n_2\, r_p^{(2)}\,; \quad p = 3, 4, ..., r \qquad (35)$$

where n_i is the ionic density. The time evolution of the population densities of the ground state and the first excited state, n_1 and n_2 respectively, can be obtained by substituting (27) and the population coefficients $r_p^{(0)}$, $r_p^{(1)}$ and $r_p^{(2)}$ into (13) with $p = 1$ and $p = 2$. We then get the two coupled first order differential equations

$$\dot{n}_1 = -S_1^{CR}\, n_e\, n_1 + M_{21}^{CR}\, n_e\, n_2 + \alpha_1^{CR}\, n_e\, n_i$$
$$\dot{n}_2 = -S_2^{CR}\, n_e\, n_2 + M_{12}^{CR}\, n_e\, n_1 + \alpha_2^{CR}\, n_e\, n_i \qquad (36)$$

where

$$S_1^{CR} = S_1 + \sum_{q=2}^{s} C_{1\to q} - \frac{1}{n_e\, Z_1} \sum_{q=3}^{s} \left(F_{q\to 1}\, n_e + A_{q\to 1} \right) Z_q\, r_q^{(1)}\,; \qquad (37)$$

$$S_2^{CR} = S_2 + F_{2\to1} + \frac{1}{n_e} A_{2\to1} + \sum_{q=3}^{s} C_{2\to q} - \\ - \frac{1}{n_e Z_2} \sum_{q=3}^{s} \left(F_{q\to2}\, n_e + A_{q\to2} \right) Z_q\, r_q^{(2)} ; \tag{38}$$

$$\alpha_1^{CR} = \alpha_1\, n_e + \beta_1 + \sum_{q=3}^{s} \left(F_{q\to1}\, n_e + A_{q\to1} \right) Z_q\, r_q^{(0)} ; \tag{39}$$

$$\alpha_2^{CR} = \alpha_2\, n_e + \beta_2 + \sum_{q=3}^{s} \left(F_{q\to2}\, n_e + A_{q\to2} \right) Z_q\, r_q^{(0)} ; \tag{40}$$

$$M_{21}^{CR} = F_{2\to1} + \frac{1}{n_e} A_{2\to1} \\ + \frac{1}{n_e Z_2} \sum_{q=3}^{s} \left(F_{q\to1}\, n_e + A_{q\to1} \right) Z_q\, r_q^{(2)} ; \tag{41}$$

$$M_{12}^{CR} = C_{1\to2} + \frac{1}{n_e Z_1} \sum_{q=3}^{s} \left(F_{q\to2}\, n_e + A_{q\to2} \right) Z_q\, r_q^{(1)} . \tag{42}$$

The coefficients S_1^{CR}, S_2^{CR} and α_1^{CR}, α_2^{CR} are similar to the hydrogenic collisional-radiative ionization rate coefficient S_{CR} (23) and recombination rate coefficient α_{CR} (24) respectively. The coefficients M_{21}^{CR} and M_{12}^{CR} have no hydrogenic counterparts. The collisional-radiative rate coefficient M_{21}^{CR} expresses the recombination which occurs in the ground state due to the neighbouring first excited state and vice versa for the collisional-radiative rate coefficient M_{12}^{CR}.

The general solution of the coupled system of equations (36) can be written as

$$n_j(t) = n_j^{SS} + n_j^{(+)} e^{-\lambda^{(+)} t} - n_j^{(-)} e^{-\lambda^{(-)} t} \tag{43}$$

where $j = 1$ or 2,

$$\lambda^{(\pm)} = \frac{n_e}{2} \left(S_1^{CR} + S_2^{CR} \pm \right. \\ \left. \pm \sqrt{\left(S_1^{CR} - S_2^{CR} \right)^2 + 4\, M_{12}^{CR}\, M_{21}^{CR}} \right), \tag{44}$$

$$n_j^{SS} = \frac{K_j^{SS}}{\lambda^{(+)}\, \lambda^{(-)}} , \tag{45}$$

$$n_j^{(\pm)} = \frac{n_j(t=0)\, \lambda^{(\pm)2} - K_j \lambda^{(\pm)} + K_j^{SS}}{\lambda^{(\pm)} \left(\lambda^{(+)} - \lambda^{(-)} \right)} , \tag{46}$$

$$K_1^{SS} = n_e^2\, n_i \left(\alpha_1^{CR}\, S_2^{CR} + \alpha_2^{CR}\, M_{21}^{CR} \right) , \tag{47}$$

$$K_2^{SS} = n_e^2\, n_i \left(\alpha_2^{CR}\, S_1^{CR} + \alpha_1^{CR}\, M_{12}^{CR} \right) , \tag{48}$$

$$K_1 = n_e \left(\alpha_1^{CR}\, n_i + S_2^{CR}\, n_1(t=0) + M_{21}^{CR}\, n_2(t=0) \right) , \tag{49}$$

$$K_2 = n_e \left(\alpha_2^{CR}\, n_i + S_1^{CR}\, n_2(t=0) + M_{12}^{CR}\, n_1(t=0) \right) . \tag{50}$$

The steady state population densities, which are obtained in the limit as $t \to \infty$, are explicitly given by

$$n_1^{SS} = \frac{\alpha_1^{CR}\, S_2^{CR} + \alpha_2^{CR}\, M_{21}^{CR}}{S_1^{CR}\, S_2^{CR} - M_{12}^{CR}\, M_{21}^{CR}}\, n_i ; \tag{51}$$

$$n_2^{SS} = \frac{S_1^{CR}\, \alpha_2^{CR} + \alpha_1^{CR}\, M_{12}^{CR}}{S_1^{CR}\, S_2^{CR} - M_{12}^{CR}\, M_{21}^{CR}}\, n_i . \tag{52}$$

4.6 Calculation of collisional and radiative rate coefficients

The results of the modelling calculations depend to a large extent on the accuracy of the collisional and radiative rate coefficients used in the CR model. The collisional rate coefficients R_n are obtained by integrating the cross-sections σ_n of the collisional processes over the free electron velocity distribution, $f(v)$:

$$R_n(T) = \int_v \sigma_n(v)\, v\, f(v)\, \mathrm{d}v . \tag{53}$$

For a Maxwellian velocity distribution of the free electrons, we have

$$f(v)\, \mathrm{d}v = \frac{4}{\sqrt{\pi}} \left(\frac{m}{2kT} \right)^{3/2} v^2\, \exp(-mv^2/2kT)\, \mathrm{d}v . \tag{54}$$

The cross-section values are obtained from experimental data, where available, and from various model and theoretical calculations that are usually fitted to semi-empirical expressions. We briefly review the expressions that have been found to be useful in CR model calculations [40].

The spontaneous transition probabilities from an upper state n to a lower state n' are given, within the electric dipole approximation, by the Einstein probability coefficient [31]

$$A_{n\to n'} = \frac{8\pi^2 e^2}{mc^3}\, \nu_{nn'}^2\, \frac{\omega_{n'}}{\omega_n}\, f_{n'\to n} \tag{55}$$

where ω_n and $\omega_{n'}$ are the statistical weights of levels n and n' respectively, $\nu_{nn'}$ is the frequency of the photon emitted as a result of the transition and $f_{n'\to n}$ is the absorption oscillator strength for the $n' \to n$ transition. The oscillator strengths can be evaluated exactly for hydrogenic ions using hypergeometric functions. Average lifetime of hydrogenic levels can be calculated from the asymptotic expression given by Millette [32]. For other elements, oscillator strengths for allowed and forbidden transitions can be evaluated using various approximate theoretical methods.

The cross-section for collisional excitation of the optically allowed transition $n' \to n$ by electron impact is given by [40]

$$\sigma_{n'\to n}(u) = 4\pi\, a_0^2\, \frac{f_{n'\to n}}{E_{n'n}^2}\, \alpha_{n'n}\, \frac{u - \phi_{n'n}}{u^2}\, \ln(1.25\, \beta_{n'n}\, u) \tag{56}$$

where $E_{n'n}$ is the threshold energy for the excitation of the $n' \rightarrow n$ transition in Rydbergs, $u = E/E_{n'n}$ is the energy of the impacting electron E in threshold units, $f_{n'\rightarrow n}$ is the absorption oscillator strength for the $n' \rightarrow n$ transition, a_0 is the Bohr radius and $\alpha_{n'n}$, $\beta_{n'n}$ and $\phi_{n'n} \leq 1$ (equal to 1 for atoms) are fit parameters depending on the transition.

The cross-section for collisional excitation of the optically forbidden transition $n' \rightarrow n$ by electron impact is given by [40]

$$\sigma_{n'\rightarrow n}(u) = 4\pi\, a_0^2 \left(\frac{n'}{n}\right)^3 \frac{\alpha_{n'n}}{E_{n'n}^2} \frac{u - \phi_{n'n}}{u^2} \qquad (57)$$

where $E_{n'n}$ is the threshold energy for the excitation of the $n' \rightarrow n$ transition in Rydbergs, $u = E/E_{n'n}$ is the energy of the impacting electron E in threshold units, a_0 is the Bohr radius and $\alpha_{n'n}$ and $\phi_{n'n}$ are fit parameters depending on the transition.

The collisional de-excitation rate coefficients are obtained from the collisional excitation rate coefficients by the principle of detailed balancing as given by (12).

The collisional ionization cross-section from state n by electron impact is given by [33, 40]

$$\sigma_n(u) = 2.66\,\pi a_0^2 \left(\frac{I_1^H}{I_n}\right)^2 \xi_n \frac{u-1}{u^2} \ln(1.25\,\beta_n\, u) \qquad (58)$$

where $I_1^H = E_1^H$ is the ionization energy of the hydrogen atom in its ground state, $I_n = E_n$ is the ionization energy of the atom or ion in state n, $u = E/I_n$ is the kinetic energy of the incident electron in units of the threshold energy for ionization from state n, ξ_n is the number of equivalent electrons in state n and β_n is a correction (fit) factor of order unity. To obtain the correct threshold law, β_n must be larger than 0.8.

The three-body recombination rate coefficients are obtained from the collisional ionization rate coefficients by the principle of detailed balancing.

The radiative recombination rate coefficients can be obtained from the photo-ionization rate coefficients by the principle of detailed balancing. The available experimental and calculated photo-ionization data are fitted to a semi-empirical function of the form [40]

$$a(u) = \frac{C}{u^p}\left[1 + \frac{b_1}{u} + \frac{b_2}{u^2} + \cdots + \frac{b_m}{u^m}\right] \qquad (59)$$

where u is the energy of the incident photon in threshold energy units, and C and b_k, $k = 1, ..., m$ are fit parameters. The parameters p and m are restricted to the range of values $0 \leq p \leq 5$ and $1 \leq m \leq 9$, and p is assigned half-integral values to simplify and facilitate the evaluation of the rate coefficient integrals.

5 Laser action in Wolf-Rayet stars

The strength of an inversely populated transition $q \rightarrow p$ ($p < q$) can be characterized by the fractional gain per unit distance, α. At the centre of a Doppler-broadened line, it is given by the following expression [34, p, 23]:

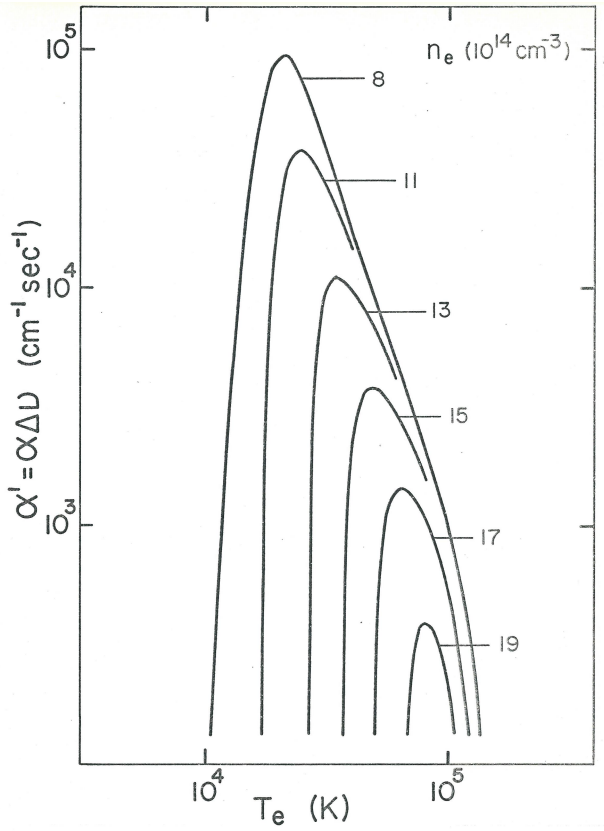

Fig. 2: Typical α' versus T_e plot for the $6f \rightarrow 5d$ transition of C IV [40, p. 249].

$$\alpha = \sqrt{\frac{\ln 2}{\pi}} \left(\frac{\omega_q A_{q\rightarrow p}}{4\pi}\right) \frac{P\,\lambda_0^2}{\Delta\nu} \qquad (60)$$

where λ_0 is the centre wavelength of the transition, $\Delta\nu$ is the linewidth, ω_q is the statistical weight of level q, $A_{q\rightarrow p}$ is the Einstein probability coefficient for spontaneous transition from level q to p, and [35]

$$P = \frac{n_q}{\omega_q} - \frac{n_p}{\omega_p}\,. \qquad (61)$$

P is a measure of the population inversion and, for laser action to be operative, $P > 0$. α is related to the intensity of a plane wave at λ_0 by the equation

$$I = I_0\, e^{\alpha L} \qquad (62)$$

where L is the length over which gain occurs. To be able to compare various transitions without needing to specify the linewidth $\Delta\nu$, we define a quantity α' given by

$$\alpha' = \alpha\,\Delta\nu \qquad (63)$$

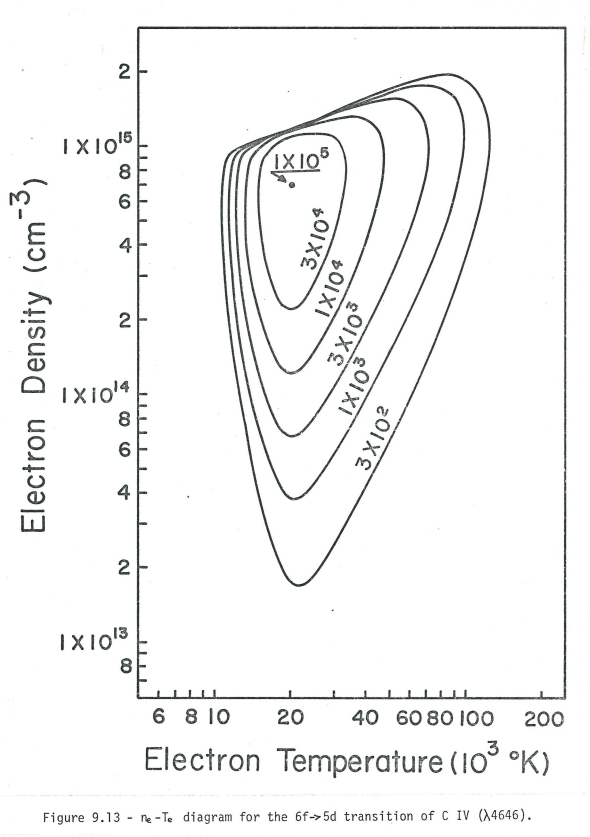

Fig. 3: Typical $n_e - T_e$ diagram showing laser gain equi-α' contours in cm^{-1} s^{-1} for the $6f \rightarrow 5d$ transition of C IV [40, p. 257].

where α is given by (60).

Model calculations starting from an initial element number density of 10^{14} cm^{-3} are performed for a grid of n_e and T_e values. The inversion is displayed on n_e, T_e plots ($n_e - T_e$ diagrams) showing contours of equal P or α' (equi-α' contours). Fig. 2 shows a typical variation of α' versus T_e for inversely populated transition $6f \rightarrow 5d$ of C IV. Fig. 3 shows a typical $n_e - T_e$ diagram with equi-α' contours for inversely populated transition $6f \rightarrow 5d$ of C IV.

On a three-dimensional plot with α' as the third axis perpendicular to both the n_e and T_e axes, the diagram would appear as a triangular pyramidal-shaped mountain with a very steep slope on the high-n_e side, a steep slope on the low-T_e side, and a gradual slope on the low-n_e, high-T_e side. Strong population inversion thus occurs only within a narrow range of values of n_e and T_e, and each transition has its own region of strong population inversion. This provides a means to classify Wolf-Rayet star parameters from their spectra.

Calculations of population inversions in astronomical plasmas cooled by adiabatic expansion have been performed on ions observed in WR stars by the following investigators. Varshni and Lam [37–39] investigated population inversions in the hydrogen-like He II ion for line λ4686 resulting from the transition $4 \rightarrow 3$ in He II.

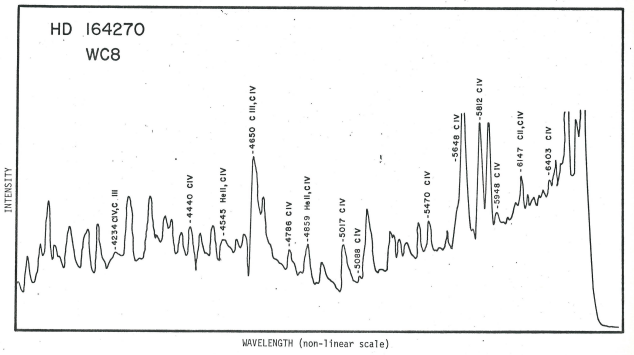

Fig. 4: Spectrum of the WC8 star HD 164270 from [36].

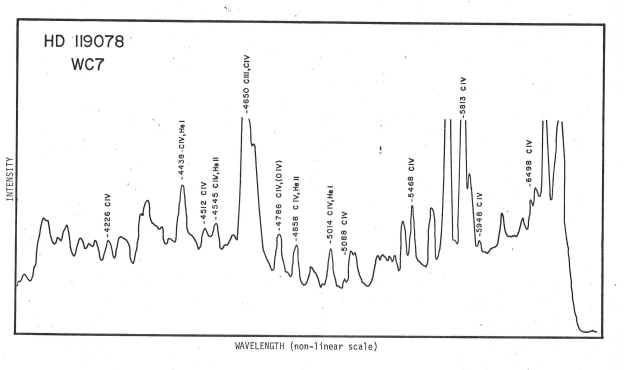

Fig. 5: Spectrum of the WC7 star HD 119078 from [36].

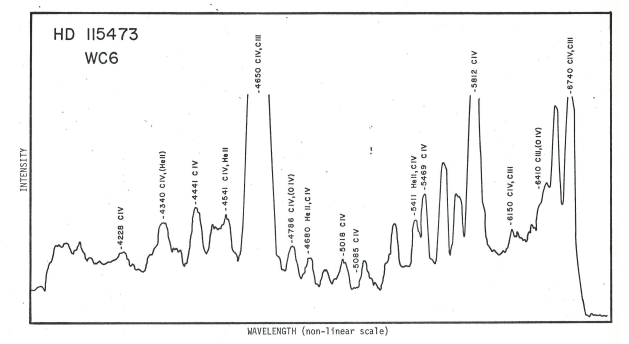

Fig. 6: Spectrum of the WC6 star HD 115473 from [36].

Millette [40] analyzed population inversions in the lithium-like ions C IV, N V and O VI. Population inversions were found to occur in many of the transitions. C IV transitions giving rise to emission lines in the visible region of the spectrum, specifically line λ4650 resulting from transitions between levels $6 \rightarrow 5$ in C IV, were investigated. The C IV $\lambda\lambda$4646, 4658 lines arising from the $6f \rightarrow 5d$ and $6g \rightarrow 5f$ transitions respectively, were found to be strongly inverted allowing laser action in plasmas cooled by adiabatic expansion.

The model calculations provide an understanding of the unusual strength of the C IV λ4650 emission line in the WC

category of Wolf-Rayet stars, as seen in Fig. 4, Fig. 5 and Fig. 6, which shows the λ4650 line becoming more and more prominent in going from a category WC8 to a WC6 Wolf-Rayet star. The lines in WC8 WR stars are relatively sharp, becoming wider and brighter in WC7 WR stars, and even wider and brighter in WC6 WR stars, indicating increasing speed of ejection and increasing laser action.

Varshni and Nasser [41,42] investigated population inversions in He I and in helium-like C III. Four transitions were investigated in the visible region of He I, λ7281 $3^1S \rightarrow 2^1P$, λ6678 $3^1D \rightarrow 2^1P$, λ5047 $4^1S \rightarrow 2^1P$ and λ4922 $4^1D \rightarrow 2^1P$, of which observationl evidence is available for λ7281 and λ6678 in WR stars. Two transitions showed appreciable population inversion in the visible region of C III: λ4650 $2s3p\,^3S \rightarrow 2p3p\,^3S$ and λ5263 $2p3p\,^3S \rightarrow 2p3s\,^3P^0$.

Millette [40] provides a detailed roadmap to calculate population inversions in hydrogenic and in the lithium-like ions N V and O VI, in addition to C IV.

6 Laser action in Quasi-Stellar Objects

The physical process of population inversions in expanding stellar atmospheres led Varshni to formulate his Plasma Laser Star (PLS) model as an explanation of the spectra of Wolf-Rayet stars and Quasi-Stellar Objects [43–48]. Radio astronomy first detected QSOs in the 1950s as anomalous objects with unexplained properties. QSO 3C 273 was the first radio source quasar for which an optical counterpart was identified in 1963. Its spectrum consisted of one strong emission line and one medium to weak strength line (λ5637, λ7588).

QSOs were named quasi-stellar because they look like stars, if not typical stars. In particular QSO spectra are dominated by a small number of very intense and wide lines that could not be readily identified with common elements. In particular, there was a lack of the expected hydrogen Lyman lines, a typical marker in most spectra. This likely provided the impetus for Schmidt [49] to assume that the observed lines in 3C 273 were the Hα and Hβ lines, red-shifted to their observed wavelength in the spectrum. This quickly became the standard approach, and ever since, astronomy and cosmology have been transformed, with everything looking like red-shifted objects, even if those red-shifts are superluminal.

Luckily, this possibility did not exist when Wolf-Rayet stars were first discovered in 1867 by astronomers Charles Wolf and George Rayet at the Paris Observatory, otherwise we would be facing an even more confusing puzzle, as hydrogen emission lines are not present in WR spectra either. As chance would have it, WR stars were investigated as stellar objects, which allowed us to eventually determine the presence of laser action in WR stellar atmospheres, which is the same process that is operating in QSO stellar atmospheres.

Banerji and Bhar [50–52] have compared the (unshifted) spectral lines of 633 QSOs discovered till August 1976, assuming they are generated by a population inversion process similar to that operating in WR stars instead of red shifts, with the laser transitions observed in laboratories till April 1976 [53]. They found that 88% of the QSO lines agreed to within 10 Å with the laser lines and 94% agreed to within 20 Å. Their assumption that QSOs are early-type stars with temperatures in the range 104–105 K implied spectral lines with asymmetric shapes and large broadening leading to errors in measurement of up to 20 Å. They pointed out the similarities between the spectra of QSOs and those of Wolf-Rayet stars, with both deficient in hydrogen. They proposed that the absorption lines of QSOs are produced in the expanding stellar atmosphere, so that they are violet-shifted as in WR stars. Under this model, they showed that 54 of 55 narrow absorption lines in QSO Q 1246-057 can be explained by assuming an average velocity of absorbing ions of 500 km/s.

Taking Quasi-Stellar Objects to be local stellar objects instead of distant galactic objects eliminates the problems associated with their currently accepted cosmological interpretation: energy source, superluminal velocities, optical variability, quasar proper motions [54, 55], quasar binary systems [56,57], naked (no nebulosity) quasars, *etc*. The properties of QSOs are similar to those of WR stars and, as stars, those are easily explainable in terms of commonly known physical processes.

7 A new star type Q and the Hertzsprung-Russell diagram

We consider the implications of Quasi-Stellar Objects as stellar objects. We need to first be more specific about the terminology used: we use the term *quasar* to refer specifically to the cosmological interpretation of Quasi-Stellar Objects, while we use the term *QSO* to refer to the stellar interpretation of Quasi-Stellar Objects. We introduce a new star type to denote QSOs: stars of type Q, similar to the Wolf-Rayet stars which are denoted as stars of type W.

The Hertzsprung-Russell diagram is extended beyond the stars of type O B towards more massive and hotter stars of type Q and W. The main sequence starts with Q W O B, followed by the standard A F G K M types of the rest of the sequence. As one moves towards star type Q, the stars become increasingly more massive, of higher temperature, with higher speeds of stellar atmosphere ejection and population inversions, with their emission spectra increasingly dominated by the lasing emission lines.

Significant work has been performed on the analysis of WR stars to understand their classification and evolution. WR stars are known to be hot, luminous objects, representative of the late stage of evolution of massive O stars. The details have been worked out over the last forty years [2, 10, 58–65] with the analysis of Wolf-Rayet stars in the Magellanic Clouds dwarf satellite galaxies of the Milky Way providing valuable information. A similar effort is required to understand the classification and evolution of stars of type Q, with the iden-

tification of unrecognized representatives in our galaxy and in the Magellanic Clouds an important step [55, 66].

8 Discussion and conclusion

In this paper, we have reconsidered the little-known but critically important physical process of laser action occurring in the stellar atmospheres of Wolf-Rayet stars and, by extension, of QSOs. We have reviewed the model used for hydrogenic and lithium-like ions in the Collisional-Radiative (non-LTE) model used to calculate the ionic energy level populations, and the existing results for He I, He II, C III and C IV. We have noted the availability of a detailed roadmap in [40] to carry out similar calculations for the lithium-like ions of interest N V and O VI.

We have reviewed the details of laser action in Wolf-Rayet stars. We have considered the historical bifurcation that resulted in the red-shift model of quasar spectra and its cosmological roots. We have also considered the evidence for the presence of laser action in QSOs as in Wolf-Rayet stars, and how taking QSOs to be local stellar objects instead of distant galactic objects eliminates the problems associated with the currently accepted cosmological interpretation.

We have introduced the terminology *quasar* to refer specifically to the cosmological interpretation of Quasi-Stellar Objects and *QSO* to refer to the stellar interpretation of Quasi-Stellar Objects. We have introduced a new star type Q for QSOs, similar to the star type W for Wolf-Rayet stars. We have expanded the Hertzsprung-Russell diagram to include more massive and hotter stars of type Q and W beyond the stars of type O B. The main sequence thus starts with stars of type Q W O B, followed by the standard types A F G K M of the rest of the sequence. Finally, we have noted the effort that will be required to understand the classification and evolution of stars of type Q, as has been achieved for Wolf-Rayet stars.

Received on December 27, 2020

References

1. Menzel D. H. Laser Action in non-LTE Atmospheres. International Astronomical Union Colloquium, Volume 2: Spectrum Formation in Stars With Steady-State Extended Atmospheres, 1970, 134–137.
2. Crowther P. A. Physical Properties of Wolf-Rayet Stars. *Annu. Rev. Astron. Astrophys.*, 2007, v. 45, 177–219. arXiv: astro-ph/0610356v2.
3. Mihalas D. Stellar Atmospheres, 2nd ed. W. H. Freeman and Co., San Francisco, 1978.
4. van der Hucht K. A. The VIIth catalogue of galactic Wolf-Rayet stars. *New Astronomy Reviews*, 2001, v. 45, 135–232.
5. van der Hucht K. A. New Galactic Wolf-Rayet stars, and candidates (Research Note), An Annex to The VIIth Catalogue of Galactic Wolf-Rayet Stars. *Astronomy and Astrophysics*, 2006, v. 458, 453–459.
6. Galactic Wolf Rayet Catalogue. V1.25, www.pacrowther.staff.shef.ac.uk/WRcat/, Aug. 2020.
7. Beals C. S. On the Nature of Wolf-Rayet Emission. *Mon. Not. Royal Ast. Soc.*, 1929, v. 90, 202–212.
8. Beals C. S. The Contours of Emission Bands in Novae and Wolf-Rayet Stars. *Mon. Not. Royal Ast. Soc.*, 1931, v. 91, 966.
9. Mihalas D. and Weibel-Mihalas B. Foundations of Radiation Hydrodynamics, corr. ed. Dover Publications, New York, 1999, pp. 627–645.
10. Abbott D. C. and Conti P. S. Wolf-Rayet Stars. *Ann. Rev. Astron. Astrophys.*, 1987, v. 25, 113–150.
11. Castor J. I. Spectral Line Formation in Wolf-Rayet Envelopes. *Mon. Not. R. Astr. Soc.*, 1970, v. 149, 111–127.
12. Castor J. I. and Van Blerkom D. Excitation of He II in Wolf-Rayet Envelopes. *Astrophys. J.*, 1970, v. 161, 485–502.
13. Castor J. I. and Nussbaumer H. On the Excitation of C III in Wolf-Rayet Envelopes. *Mon. Not. R. Astr. Soc.*, 1972, v. 155, 293–304.
14. Gudzenko L. L., Shelepin L. A. Negative Absorption in a Nonequilibrium Hydrogen Plasma. *Zh. Eksp. Teor. Fiz.*, 1963, v. 45, 1445–1449. *Sov. Phys. JETP*, 1964, v. 18, 998–1000.
15. Gudzenko L. L., Shelepin L. A. Amplification in Recombination Plasma. *Dokl. Akad. Nauk. SSSR*, 1965, v. 160, 1296–1299. *Sov. Phys. - Dokl.*, 1965, v. 10, 147.
16. Gudzenko L. L., Filippov S. S., Shelepin L. A. Rapid Recombination of Plasma Jets. *Zh. Eksp. Teor. Fiz.*, 1966, v. 51, 1115–1119. *Sov. Phys. JETP*, 1967, v. 24, 745–748.
17. Gudzenko L. I., Mamachun A. T., and Shelepin L. A. *Zh. Tekh. Fiz.*, 1967, v. 37, 833. *Sov. Phys. - Tech. Phys.*, 1967, v. 12, 598.
18. Gudzenko L. L., Shelepin L. A., Yakovlenko S. I. Amplification in recombining plasmas (plasma lasers). *Usp. Fiz. Nauk*, 1974, v. 114, 457. *Sov. Phys. - Usp.*, 1975, v. 17, 848.
19. Gol'dfarb V. M., Il'ina E. V., Kostygova I. E., Luk'yanov G. A. and Silant'ev, V. A. *Opt. Spektrosk.*, 1966, v. 20, 1085. *Optics and Spectrosc.*, 1969, v. 20, 602.
20. Gol'dfarb V. M., Il'ina E. V., Kostygova I. E. and Luk'yanov G. A. *Opt. Spektrosk.*, 1969, v. 27, 204. *Optics and Spectrosc.*, 1969, v. 27, 108.
21. Bates D. R., Kingston A. E. and McWhirter R. W. P. *Proc. Roy. Soc.*, 1962, v. A267, 297.
22. Bates D. R., Kingston A. E. and McWhirter R. W. P. *Proc. Roy. Soc.*, 1962, v. A270, 155.
23. Bates D. R. and Kingston A. E. *Planet. Space Sci.*, 1963, v. 11, 1.
24. McWhirter R. W. P. and Hearn A. G. *Proc. Phys. Soc.*, 1963, v. 82, 641.
25. Drawin H. W. and Emard F. Instantaneous Population Densities of the Excited Levels of Hydrogen Atoms, Hydrogen-like Ions, and Helium Atoms in Optically Thin and Thick Non-LTE Plasmas. Euratom-C.E.A. Report No. EUR-CEA-FC-534, 1970.
26. Gordiets B. F., Gudzenko L. I. and Shelepin L. A. Relaxation processes and amplification of radiation in a dense plasma. *Zh. Eksp. Teor. Fiz.*, 1968, v. 55, 942. *Sov. Phys. - JETP*, 1969, v. 28, 489.
27. Norcross D. W. and Stone P. M. *J. Quant. Spectrosc. Radiat. Transfer*, 1968, v. 8, 655.
28. Unsöld A. The New Cosmos, 2nd edition. Springer-Verlag, Berlin, 1977.
29. Griem H. R. Plasma Spectroscopy. McGraw-Hill, New York, 1964.
30. House L. L. *Astrophys. J. Suppl.*, 1964, v. 8, 307.
31. Menzel D. H. and Pekeris C. L. *Mon. Not. Roy. Astron. Soc.*, 1935, v. 96, 77.
32. Millette P. A. and Varshni Y. P. New Asymptotic Expression for the Average Lifetime of Hydrogenic Levels. *Can. J. Phys.*, 1979, v. 57 (3), 334–335.
33. Drawin H. W. Collision and Transport Cross-Sections. Euratom-C.E.A. Report No. EUR-CEA-FC-383, 1966.
34. Willett C. S. Gas Lasers: Population Inversion Mechanisms. Pergamon Press, New York, 1974.

35. Lengyel B. A. Introduction to Laser Physics. John Wiley, New York, 1966.
36. Smith H. J. Ph.D. Thesis, Dept. of Astronomy, Harvard University, Cambridge, 1955.
37. Varshni Y. P., Lam C. S. Emission Line 4686 in the Quasi-Stellar Objects. *J. Roy.Astron. Soc. Canada*, 1974, v. 68, 264.
38. Varshni Y. P., Lam C. S. Laser Action in Stellar Envelopes. *Bull. Amer. Astron. Soc.*, 1975, v. 7, 551.
39. Varshni Y. P., Lam C. S. Laser Action in Stellar Envelopes. *Astrophys. Space Sci.*, 1976, v. 45, 87.
40. Millette P. A. Laser Action in C IV, N V, and O VI Plasmas Cooled by Adiabatic Expansion. University of Ottawa, Ottawa, ON, 1980. LaTeX typeset, researchgate.net/publication/283014713, 2015.
41. Nasser R. M. Population Inversion in He I and C III in Recombining Plasmas. University of Ottawa, Ottawa, ON, 1986.
42. Varshni, Y. P., Nasser R. M. Laser Action in Stellar Envelopes II. He I. *Astrophys. Space Sci.*, 1986, v. 125, 341.
43. Varshni Y. P. Laser Action in Quasi-Stellar Objects? *Bull. Amer. Phys. Soc.*, 1973, v. 18, 1384.
44. Varshni Y. P. No Redshift in Quasi-Stellar Objects. *Bull. Amer. Astron. Soc.*, 1974, v. 6, 213.
45. Varshni Y. P. The Redshift Hypothesis and the Plasma Laser Star Model for Quasi-Stellar Objects. *Bull. Amer. Astron. Soc.*, 1974, v. 6, 308.
46. Varshni Y. P. Alternative Explanation for the Spectral Lines Observed in Quasars. *Astrophys. Space Sci.*, 1975, v. 37, L1.
47. Varshni Y. P. Electron Density in the Emission-Line Region of Wolf-Rayet Stars. *Astrophys. Space Sci.*, 1978, v. 56, 385.
48. Varshni Y. P. The Physics of Quasars. *Phys. Canada*, 1979, v. 35, 11.
49. Schmidt M. 3C 273: A Star-Like Object with Large Red-Shift. *Nature*, 1963, v. 197, 1040.
50. Banerji S. and Bhar G. C. Plasma laser star model of QSOs. *Astrophysics and Space Science*, 1978, v. 56, 443–451.
51. Banerji S. and Bhar G. C. Analysis of the plasma laser star model of QSOs. *Astrophysics and Space Science*, 1979, v. 61, 337–347.
52. Banerji S., Bhar G. C. and Mukherji P, K. Are QSOs local objects? I. A new interpretation of the emission and absorption spectra of a few QSOs. *Astrophysics and Space Science*, 1982, v. 87, 217–236.
53. Willett, C. S. Laser Lines in Atomic Species. In: Progress in Quantum Electronics, Vol. 1, Part 5, Pergamon, 1971.
54. Luyten W. J. A Search for Faint Blue Stars. Paper 50, University of Minnesota Observatory, Minneapolis, 1969.
55. Varshni Y. P. Proper Motions and Distances of Quasars. *Speculations in Science and Technology*, 1982, v. 5 (5), 521–532.
56. Mortlock D. J., Webster R. L. and Francis P. J. Binary Quasars. *Mon. Not. R. Astron. Soc.*, 1999, v. 309, 836–846.
57. Hennawi J. F., et al. Binary Quasars in the Sloan Digital Sky Survey: Evidence for Excess Clustering on Small Scales. *Astronomical Journal*, 2006, v. 131, 1–23.
58. Conti P. S. and Garmany C. D., De Loore C. and Vanbeveren D. The Evolution of Massive Stars: The Numbers and Distribution of O Stars and Wolf-Rayet Stars. *Astrophys. J.*, 1983, v. 274, 302–312.
59. Humphreys R. M. and Nichols M., Massey P. On the Initial Masses and Evolutionary Origins of Wolf-Rayet Stars. *Astron. J.*, 1985, v. 90, 101–108.
60. Conti P. S. and Vacca W. D. The Distribution of Massive Stars in the Galaxy: I. Wolf-Rayet Stars. *Astron. J.*, 1990, v. 100, 431–444.
61. Langer N., Hamann W.-R., Lennon M., Najarro F., Pauldrach A.Ẇ. A. and Puls J. Towards an understanding of very massive stars. A new evolutionary scenario relating O stars, LBVs [Luminous Blue Variables] and Wolf-Rayet stars. *Astron. Astrophys.*, 1994, v. 290, 819–833.
62. Crowther P. A., Smith L. J., Hillier D. J. and Schmutz W. Fundamental parameters of Wolf-Rayet stars. III. The evolutionary status of WNL [WN7 to WN9] stars. *Astron. Astrophys.*, 1995, v. 293, 427–445.
63. Hainich R., Rühling U., Todt H., Oskinova L. M., Liermann A., Gräfener G., Foellmi C., Schnurr O. and Hamann W.-R. The Wolf-Rayet stars in the Large Magellanic Cloud. A comprehensive analysis of the WN class. *Astronomy & Astrophysics*, 2014, v. 565, A27, 1-62.
64. Koesterke L. and Hamann W.-R. Spectral analyses of 25 Galactic Wolf-Rayet stars of the carbon sequence. *Astron. Astrophys.*, 1995, v. 299, 503–519.
65. Barlow M. J. and Hummer D. J. The WO Wolf-Rayet stars. *Symposium – International Astronomical Union*, 1982, v. 99, 387–392.
66. Varshni Y. P. O VI and He II Emission Lines in the Spectra of Quasars. *Astrophys. Space Sci.*, 1977, v. 46, 443.